Received: 19 August 2019 | Revised: 13 September 2019 | Accepted: 13 September 2019

DOI: 10.1111/jace.16803

ORIGINAL ARTICLE

Journal of the American Ceramic Society

Tetrahedral amorphous boron nitride: A hard material

Murat Durandurdu

Department of Materials Science & Nanotechnology Engineering, Abdullah Gül University, Kayseri, Turkey

Correspondence
Murat Durandurdu, Department of Materials Science & Nanotechnology Engineering, Abdullah Gül University, Kayseri 38080, Turkey.
Email: murat.durandurdu@agu.edu.tr

Funding information
Türkiye Bilimsel ve Teknolojik Araştirma Kurumu, Grant/Award Number: 117M372

Abstract

We generate a tetrahedrally coordinated amorphous boron nitride (BN) model by means of first principles molecular dynamics calculations and report its mechanical and electrical properties in detail. The amorphous configuration is almost free from chemical disorder and consists of about 20% coordination defects, similar to tetrahedral (diamond-like) amorphous carbon. Its theoretical band gap energy is about 2.0 eV, less than 4.85 eV estimated for cubic BN. The bulk modulus and Vickers hardness of tetrahedral amorphous BN are computed as 206 GPa and 28-35 GPa, respectively. Based on these findings, we propose that tetrahedral noncrystalline BN can serve as electronic and hard materials as well.

KEYWORDS

amorphous, boron nitride

1 | INTRODUCTION

Boron nitride (BN), being a wide band gap semiconductor ceramic, possesses remarkable properties and hence has various high-tech applications. BN has four different crystalline forms.[1–4] The hexagonal (h-BN) and rhombohedral (r-BN) crystals with threefold coordination have a two-dimensional (2D) structure while the cubic (c-BN) and wurtzite (w-BN) phases with fourfold tetrahedral coordination have a three-dimensional (3D) structure. Both 3D-phases can be attainable by pressurizing of h-BN and r-BN at room or high temperatures. Due to their high hardness, these 3D-crystals are considered as superhard materials.

Amorphous form of BN with sp^2 hybridization can be easily produced by several experimental methods such as high frequency plasma-assisted chemical vapor deposition, ball milling etc.[5–18] Yet its properties are still needed to be explored. Amorphous cubic BN layers were also fabricated by the reactive pulse plasma method.[19] However, to the best of our knowledge, the atomic structure and the electrical and mechanical properties of tetrahedrally coordinated amorphous BN have not been revealed in any study so far. It should be pointed out here that BN forms structures, similar to those of carbon and tetrahedral amorphous carbon (ta-C) shows remarkable features. Therefore, it is possible that tetrahedral amorphous BN can also possess extraordinary properties as in the crystals. In this work, we investigate the properties of a tetrahedrally coordinated amorphous BN model using ab initio molecular dynamics (MD) calculations. The model is generated using the melt-quench method and has a few coordination defects and useful elecrical and mechanical features.

2 | METHODOLOGY

An ab initio code[20] within a pseudopotential method[21] and a generalized gradient approximation (GGA)[22,23] was used to model tetrahedral amorphous BN. We did the Brillion zone integration at Γ point. Double-zeta basis functions were employed for the MD simulations whereas double-zeta plus polarization basis sets were applied for the geometry optimization. c-BN having 216 atoms and the lattice parameter of a = 10.86 Å was used as a starting structure and the NVT ensemble was chosen to perform MD simulations. Each MD time step was set to be 1.0 fs. c-BN was exposed to 8500 K for 2.0 ps and later the structure was quickly cooled to 5500 K. At this temperature, it was equilibrated about 20.0 ps. The well-equilibrated configuration was then cooled using a quenching rate of 2×10^{13} K/s. For this quenching rate, the system remained disordered at 4900 K but it

transformed to a crystalline structure at 4800 K as shown in Figure 1. Starting from 4900 K, we tried several cooling rates (4×10^{13}-2×10^{14}K/s) but observed the crystallization or crystalline-like phases. We only perceived a disordered structure at 300 K for the cooling rate of 4×10^{14} K/s. This disordered structure was finally relaxed using a variable cell conjugate gradient relaxation technique in which both atomic positions and lattice parameters were optimized.

3 | RESULTS

Figure 2 shows the partial pair correlation functions (PPCFs) of the optimized amorphous model along with those of c-BN at ambient pressure. The mean B–N bond distance is found to be 1.56 Å for the crystal and 1.55 Å for the amorphous configuration. These values well agree with the experimental bond separation of 1.57 Å in c-BN.[24] The first sharp peak of B–B and N–N correlations is located at 2.56 Å for the crystal and 2.58 Å for the amorphous network. Again they accord with the experimental value of 2.56 Å reported for c-BN.[24] The presence of a weak peak at 1.69 Å for the B–B pair and 1.55 Å for the N–N correlation, which are the main distinction between amorphous and crystalline states for the short-range order, suggests the formation of some homopolar (wrong) bonds in the amorphous network but their fraction indeed is very small and hence the model can be considered as almost free from chemical disorder.

We next analyze the coordination number (CN) and coordination distribution using the first minimum of the PPCFs (B–B = 1.84 Å, B–N = 2.14 Å and N–N = 1.90 Å). The mean CN of both B and N atoms is 3.79. The average N–N and B–B CNs are 0.09, implying the presence of a negligible amount of wrong bonds in the noncrystalline state. In the model, 80% of B and N atoms show fourfold tetrahedral coordination while the rest exhibit only threefold coordination. These values are indeed comparable with ta-C that presents about 60%–80% sp^3 bonding.[25] The chemical environmental distribution given Table 1 can provide more information about the disordered BN structure. One can see that B–N_4

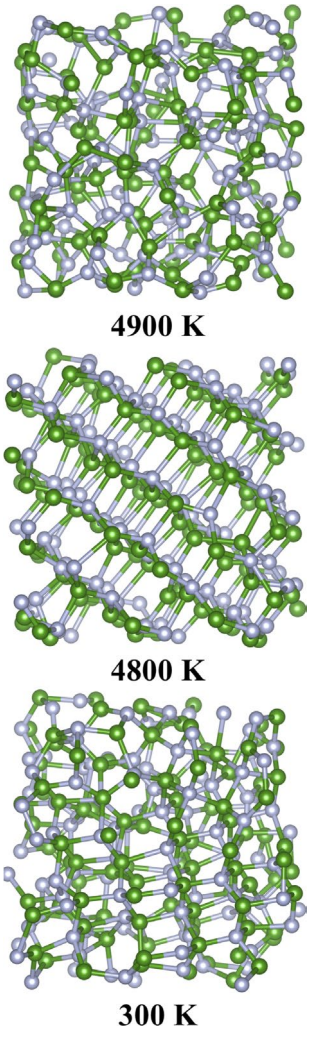

FIGURE 1 Ball-stick representation of boron nitride systems [Color figure can be viewed at wileyonlinelibrary.com]

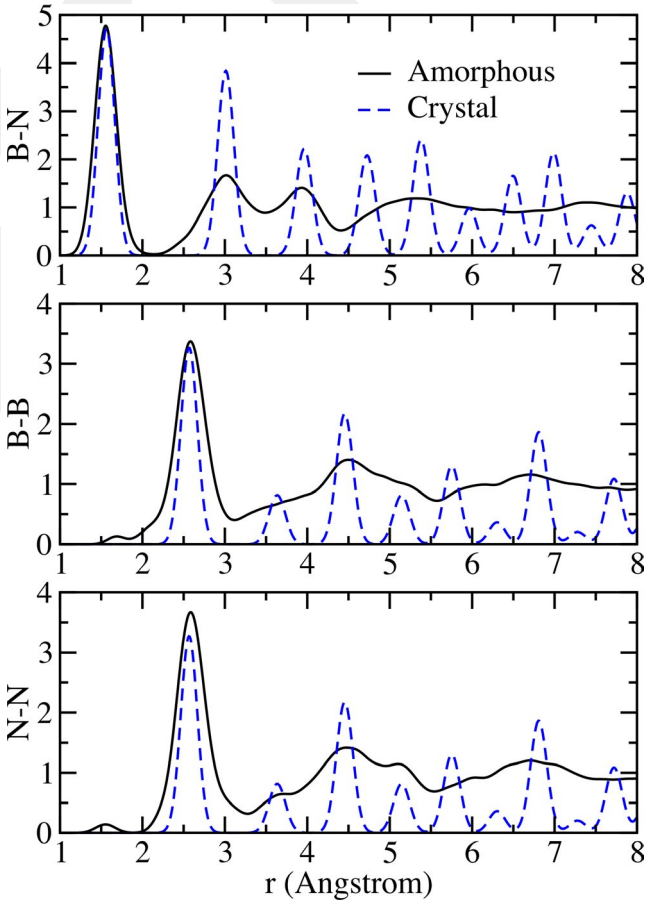

FIGURE 2 Partial pair correlation functions of the cubic and tetrahedral amorphous forms of boron nitride [Color figure can be viewed at wileyonlinelibrary.com]

TABLE 1 Chemical identities of B and N atoms in the tetrahedral amorphous BN model

B		N	
N_4	74.074%	B_4	71.296%
N_3	16.667%	B_3	19.444%
BN_3	5.556%	B_3N	8.333%
BN_2	3.704%	B_2N	0.926%

and N–B_4 units are the most predominant ones in the network followed by B–N_3 and N–B_3 type motifs and that some tetrahedrally coordinated configurations such as B–BN_3 and N–NB_3 involve with a homopolar bond. From the table one can also notice that the equal number of B and N atoms includes a wrong bond.

To provide more knowledge concerning the local of the noncrystalline state, we next examine the bond angle distributions and give them in Figure 3. Both B–N–B and N–B–N angles produce a main peak at around 109^o close to the ideal tetrahedral angle of 109.5^o, supporting the tetrahedral character of the network. The angles near 90^o are due to the four membered rings formed in the disordered state. The four membered rings were also observed in a hexagonal-like amorphous model generated in our previous study.[26]

We perform the ring statistical analysis to have some information about the topological connectivity of the amorphous state and provide the analysis in Figure 4. The six-membered rings, only ring in cubic-BN, are the most frequent one in the amorphous configuration followed by eight-membered rings. This again supports the tetrahedral

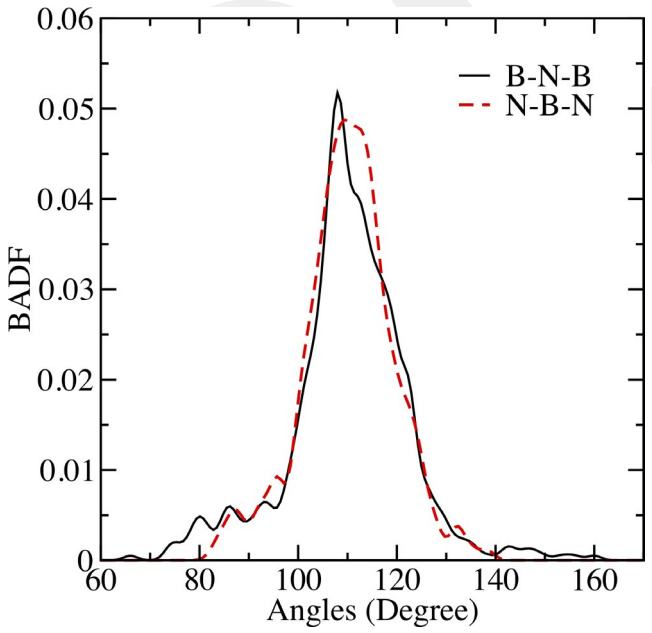

FIGURE 3 Bond angle distribution functions (BADFs) of tetrahedral amorphous boron nitride [Color figure can be viewed at wileyonlinelibrary.com]

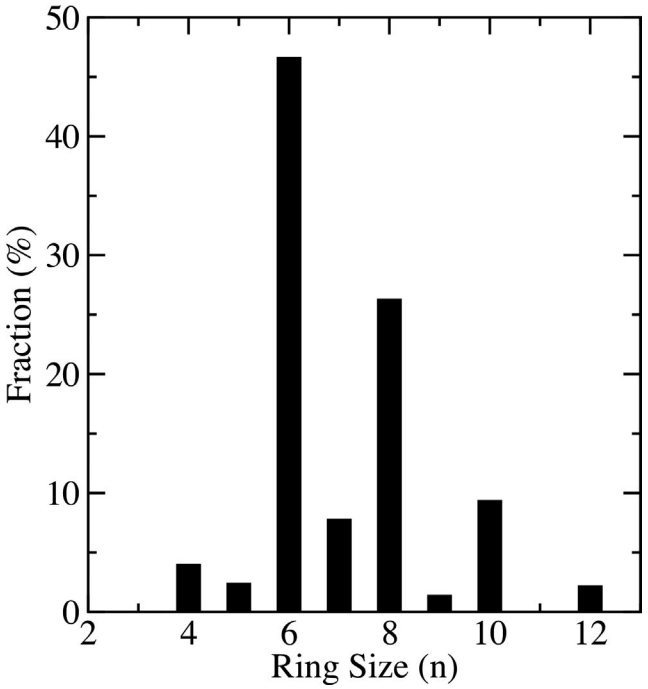

FIGURE 4 Ring distribution for the amorphous form of tetrahedral boron nitride

nature of the amorphous network. The model presents some odd membered rings due to the existence of B–B and N–N homopolar bonds and a small amount of four membered rings. As mentioned above, such four membered rings were also witnessed in our 2D structured amorphous model.[26] It should be also noted here that ta-C presents four-membered rings as well.[27] Yet when the ring formation is considered, the basic difference between these two tetrahedral forms is the lack of three-membered rings in tetrahedral amorphous BN, in a stark contrast to ta-C.

Some applications of BN phases require the knowledge of their electronic properties. Here by calculating total and partial electron density of states (given in Figure 5), we reveal the electronic structure of tetrahedral amorphous BN and compare it with that of c-BN. The forbidden energy band gap of c-BN is projected to be ~4.85 eV that is, as expected, smaller than the experimental data of about 6.0-6.4 eV[28–31] due to the limitation of DFT-GGA calculations. For the noncrystalline network, the estimated forbidden band gap is ~2.0 eV. The energy band gap of c-BN is underestimated about 20%-24%, and by assuming the same underestimation for the noncrystalline state, we speculate that the experimental band gap energy of the terahedral amorphous phase could be around 2.5 eV. To provide further knowledge about their electronic structure, we analyze the partial electron density of states. The valence band near the Fermi energy has a main contribution from N-p states while the conduction band has a major contribution from B-p states, similar to h-BN.

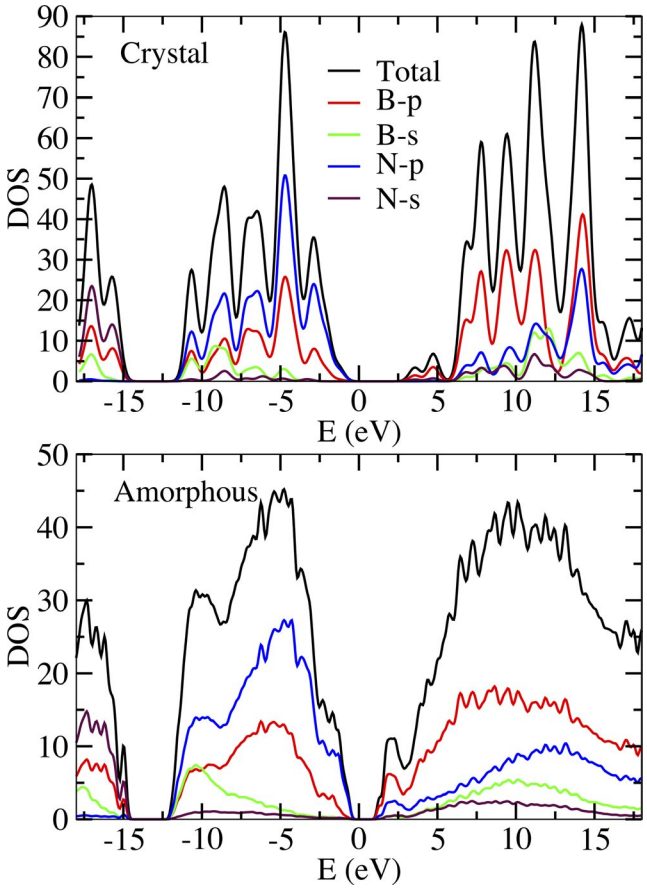

FIGURE 5 Total and partial electron density of states of cubic and tetrahedral amorphous forms of boron nitride [Color figure can be viewed at wileyonlinelibrary.com]

The band tail states of amorphous materials present some signature of localization because of the presence of both topological and chemical disorders in the networks. We characterize the nature of the band tail states using inverse participation ratio (IPR) given by

$$\mathrm{IPR}\left(\psi_j\right) = N\sum_{i=1}^{N} a_i^{m4} \Big/ \left(\sum_{i=1}^{N} a_i^{m2}\right)^2$$

where $\psi_m = \sum_{i=1}^{N} a_i^m \phi_i$ is the m^{th} eigenstate and N corresponds to the number of atoms. The IPR of the noncrystalline phase is offered in Figure 6. The valance states close to the Fermi level are quite localized because of their high IPR values while the conduction tails are weakly localized because of their low IPR values, signifying an unequal localization near the Fermi level. Such a feature might be used to propose suitable type impurities for the amorphous model.[32] Namely moving the Fermi energy to the valence band could be tougher than moving the energy to the conduction band and consequently n-type doping is more suitable than p-type doping.

c-BN ranks the second hardest material after diamond. In order to see whether its amorphous form also presents the same features, we focus on its mechanical properties in details. In order to calculate bulk modulus (K) of the phases, we study their energy-volume relation (see Figure 7) and fit it to the third-order Birch-Murnaghan equation of states.

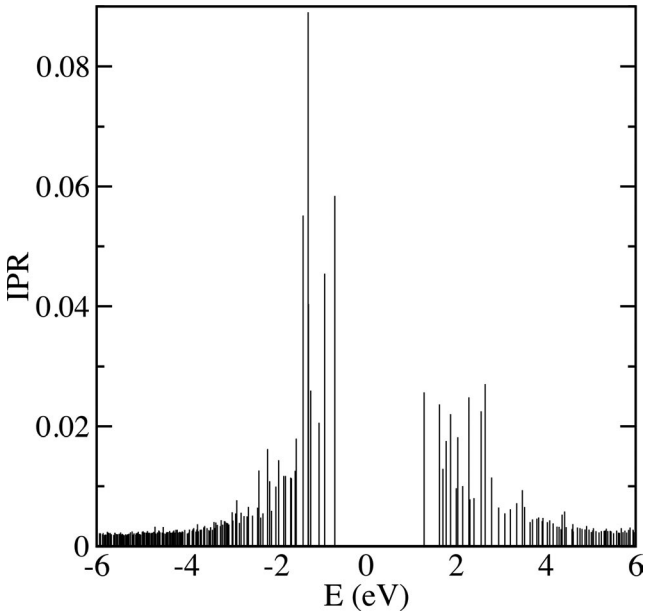

FIGURE 6 Inverse participation ratio (IPR) of tetrahedral amorphous boron nitride

$$E(V) = E_o + \frac{9V_O K}{16}\left\{\left[\left(\frac{V_O}{V}\right)^{\frac{2}{3}} - 1\right]^3 K' + \left[\left(\frac{V_O}{V}\right)^{\frac{2}{3}} - 1\right]^2 \left[6 - 4\left(\frac{V_O}{V}\right)^{\frac{2}{3}}\right]\right\}.$$

From the fitting, the bulk modulus is projected to be 361 GPa for the crystalline phase and 206 GPa for the disordered network. So a noticeable decrease in the bulk modulus is observed by amorphization in BN. The estimated bulk modulus for the c-BN is fairly agrees with the earlier predictions of 363-410 GPa.[33]

From the equation of state, the equilibrium volume (V_0) of the crystalline and amorphous structures is predicted to be 6.033 and 6.684 Å^3/atom, respectively. Accordingly amorphization results in about 11% volume swelling in BN. The relative energy difference between two forms of BN at the equilibrium is 0.488 eV/atom.

Since the Young's modulus (E) can be straightforwardly calculated from the stress-strain relation,

$$E = \frac{\text{Stress}}{\text{Strain}} = \frac{\sigma}{\epsilon_{\text{applied}}}$$

both tetrahedral BN phases are uniaxially compressed along the diagonal lattice vectors' direction (due to the cubic

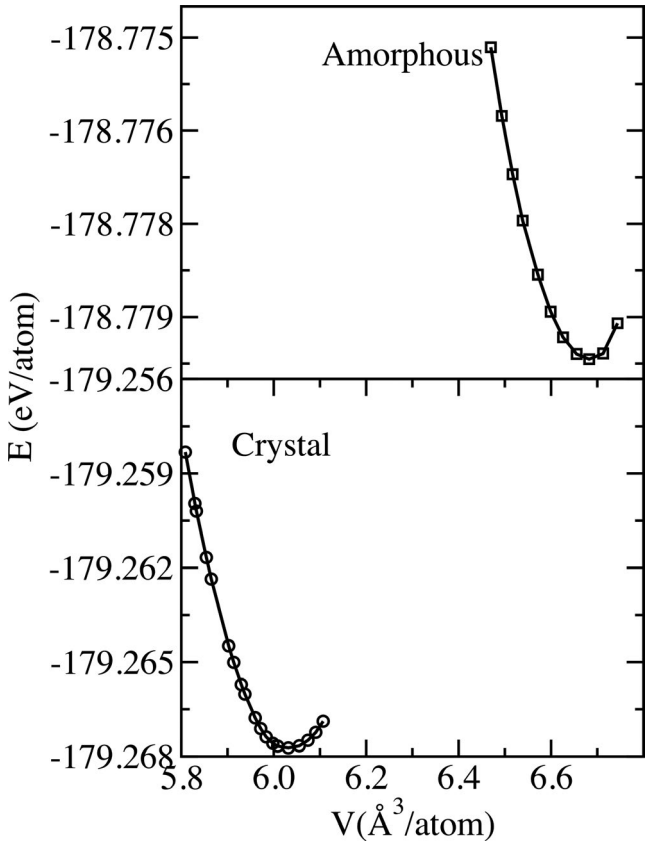

FIGURE 7 Energy-volume relation of the cubic and tetrahedral amorphous forms of boron nitride

symmetry, c-BN is compacted along [100] direction only) and the stress-strain relations are monitored. From the best fitting, E is found to be 754 GPa for the crystal and 443 GPa (the average value) for the disordered network. The E value obtained for the crystal is indeed parallel to the prior results of 587 ± 30 GPa-909 GPa[34–36]

We also attain the lateral strain ($\varepsilon_{\text{lateral}}$)—applied strain ($\varepsilon_{\text{applied}}$) relation from the uniaxial compression simulations and calculate the Poisson's ratio (ν) using the following equation,

$$\nu = -\frac{\varepsilon_{\text{lateral}}}{\varepsilon_{\text{applied}}}$$

to be 0.16 for the crystal and 0.18 for the disordered network. Again our value for the crystal agrees with data of 0.11-0.17[34,37] available in the literature.

The next definition

$$\mu = \frac{E}{2(1+\nu)}$$

leads the shear modulus (μ) to be 325 GPa for c-BN and 187 GPa for the noncrystalline model. Our estimation for c-BN is in agreement with 275-405 GPa.[37]

The Vickers hardness (H_v) is computed using three different equations,[38–40]

$$H_v = 0.151\mu,$$

$$H_v = 2\left(\frac{\mu}{n^2}\right)^{0.585} - 3(\text{Gpa}),$$

$$H_v = 0.92\left(\frac{1}{n}\right)^{1.137}(\mu)^{0.708}.$$

For c-BN, these equations give its Vickers hardness to be around 49 GPa, in agreement with the earlier predictions of 40-75 GPa.[41,42] For the amorphous state, its hardness is calculated as 28-35 GPa. Consequently a noticeable reduction is witnessed in the Vickers hardness accompanied by amorphization. Nonetheless the tetrahedral amorphous form of BN can still be categorized as a hard material.

4 | CONCLUSIONS

A tetrahedral amorphous BN network is modeled using a constant volume ab initio simulations and its mechanical and electrical properties are reported for the first time. The noncrystalline configuration presents almost no chemical disorder. Yet similar to ta-C, it shows coordination defects, in particular, under-coordinated atoms. It is a semiconducting material with a GGA energy band gap of about 2.0 eV, which is noticeably less than 4.85 eV projected for c-BN. Its bulk modulus and Vickers hardness are estimated as about 206 GPa and 28-35 GPa, respectively, signifying that tetrahedral amorphous BN can also serve as a hard material. Yet we need to point out here that tetrahedral amorphous BN can have different local structures (number coordination defects or chemical defects, etc) depending on experimental preparation procedures and hence it can possess different mechanical and electrical properties and might offer various high-tech applications.

ACKNOWLEDGMENTS

This study was supported by the Scientific and Technological Research Council of Turkey (TÜBİTAK) under grant number 117M372. The simulations were run on the TÜBİTAK ULAKBİM, High Performance and Grid Computing Center (TRUBA resources).

ORCID

Murat Durandurdu https://orcid.org/0000-0001-5636-3183

REFERENCES

1. Paine RT, Narula CK. Synthetic routes to boron nitride. Chem Rev. 1990;90:73–91.

2. Matsui Y, Sekikawa Y, Sato T, Ishii T, Isakosawa S, Shii K. Formations of rhombohedral boron nitride, as revealed by TEM-electron energy loss spectroscopy. J Mater Sci. 1981;16:1114–6.
3. Wentorf RH Jr. Synthesis of the cubic form of boron nitride. J Chem Phys. 1961;34:809–12.
4. Bundy FP, Wentorf RH Jr. Direct transformation of hexagonal boron nitride to denser forms. J Chem Phys. 1963;38:1144–9.
5. Hamilton EJ, Dolan SE, Mann CM, Colijn HO, McDonald CA, Shore SG. Preparation of amorphous boron nitride and its conversion to a turbostratic, tubular form. Science. 1993;260:659–61.
6. Lorenz H, Orgzall I. In situ observation of the crystallization of amorphous boron nitride at high pressures and temperatures. Scr Mater. 2005;52:537–40.
7. Zedlitz R, Heintze M, Schubert MB. Properties of amorphous boron nitride thin films. J Non-Cryst Solids. 1996;198:403–6.
8. Huang JY, Yasuda H, Mori H. HRTEM and EELS studies on the amorphization of hexagonal boron nitride induced by ball milling. J Am Ceram Soc. 2000;83:403–9.
9. Weissmantel S, Reisse G, Keiper B, Schulze S. Microstructure and mechanical properties of pulsed laser deposited boron nitride films. Diamond Relat Mater. 1999;8:377–81.
10. Ketchum DR, DeGraffenreid AL, Niedenzu PM, Shore SG. Synthesis of amorphous boron nitride from the molecular precursor ammonia monochloroborane. J Mater Res. 1999;14:1934–8.
11. Li D, Zhang C, Li B, Cao F, Wang S, Liu K, et al. Low-cost preparation of boron nitride ceramic powders. J Wuhan Univ Technol Mater Sci Ed. 2012;27:534–7.
12. Taniguchi T, Kimoto K, Tansho M, Horiuchi S, Yamaoka S. Phase transformation of amorphous boron nitride under high pressure. Chem Mater. 2003;15:2744–51.
13. Werbowy A, Szmidt J, Sokołowska A, Olszyna A. Heterojunctions of amorphous wide band gap nitrides and silicon. Diamond Relat Mater. 1998;7:397–401.
14. Kayed K, Abdeh H, Alshoufi K. Effect of nitrogen plasma after glow on amorphous boron nitride thin films deposited by laser ablation. Int J Chem Tech Res. 2014;6:2719–24.
15. Singhal SK, Park JK. Synthesis of cubic boron nitride from amorphous boron nitride containing oxide impurity using Mg–Al alloy catalyst solvent. Cryst Growth Des. 2004;260:217–22.
16. Cao F, Liu K, Fang Z, Wang S. Hydrolysis mechanism of borazine-derived boron nitride pyrolysized below 1200°C. J Mater Sci Technol. 2012;28:956–60.
17. King SW, French M, Bielefeld J, Jaehnig M, Kuhn M, French B. X-ray photoelectron spectroscopy investigation of the Schottky barrier at a-BN:HCu interfaces. Electrochem Solid-State Lett. 2011;14:H478–H479.
18. King SW, French M, Bielefeld J, Jaehnig M, Kuhn M, Xu G, et al. Valence band offset at the amorphous hydrogenated boron nitride-silicon (100) interface. Appl Phys Lett. 2012;101:042903–5.
19. Werbowy A, Szmidt J, Sokolowska A, Olszyna A, Mitura S. Fabrication and properties of Mo contacts to amorphous cubic boron nitride (a-cBN) layers. Diamond Relat Mater. 1996;5:1017–20.
20. Ordejón P, Artacho E, Soler JM. Self-consistent order-N density- functional calculations for very large systems. Phys Rev B. 1996;53:R10441–4.
21. Troullier N, Martins JL. Efficient pseudopotentials for plane-wave calculations. Phys Rev B. 1991;43:1993–2006.
22. Becke AD. Density functional exchange energy approximation with correct asymptotic behavior. Phys Rev A. 1988;38:3098–3100.
23. Lee C, Yang W, Parr RG. Development of the Colle-Salvetti correlation-energy formula into a functional of the electron density. Phys Rev B. 1988;37:785–9.
24. Kumashiro Y, editor. Electric refractory materials. New York, NY: Taylor & Francis; 2000.
25. Mari D, Miguel L, Nebel C, editors. Comprehensive hard materials, vol. 1; p. 101–39. Oxford, UK: Elsevier; 2014.
26. Durandurdu M. Hexagonal nanosheets in amorphous BN: a first principles study. J Non-Crystal Solids. 2015;427:41–5.
27. McCulloch DG, McKenzie DR, Goringe CM. Ab initio simulations of the structure of amorphous carbon. Phys Rev B. 2000;61:2349–55.
28. Fomichev VA, Rumsh MA. Investigation of X-ray spectra of hexagonal and cubic boron nitride. J Phys Chem Solids. 1968;29:1015–24.
29. Miyata N, Moriki K, Mishima O, Fujisawa M, Hattori T. Optical constants of cubic boron nitride. Phys Rev B. 1989;40:12028–9.
30. Evans DA, McGlynn AG, Towlson BM, Gunn M, Jones D, Jenkins TE, et al. Determination of the optical band-gap energy of cubic and hexagonal boron nitride using luminescence excitation spectroscopy. J Phys: Condens Matter. 2008; 20:075233–339.
31. Chrenko RM. Ultraviolet and infrared spectra of cubic boron nitride. Solid State Commun. 1974;14(6):511–5.
32. Robertson J. Physics of amorphous conducting oxides. J Non-Cryst Solids. 2008;354:2791–5.
33. Zhang JS, Bass JD, Taniguchi T, Goncharov AF, Chang YY, Jacobsen SD. Elasticity of cubic boron nitride under ambient conditions. J Appl Phys. 2011;109:063521–5.
34. Zhang F, Guo Y, Song Z, Chen G. Deposition of high quality cubic boron nitride films on nickel substrates. J Appl Phys Lett. 1994;65:971–3.
35. Mirkarimi PB, Medlin DL, McCarty KF, Dibble DC, Clift WM, Knapp JA, et al. The synthesis, characterization, and mechanical properties of thick, ultrahard cubic boron nitride films deposited by ion-assisted sputtering. J Appl Phys. 1997;82:1617–25.
36. Grimsditch M, Zouboulis ES, Polian A. Elastic constants of boron nitride. J Appl Phys. 1994;76:832–4.
37. D'Evelyn MP, Taniguchi T. Elastic properties of translucent polycrystalline cubic boron nitride as characterized by the dynamic resonance method. Diamond Relat Mater. 1999;8:1522–6.
38. Teter DM. Computational alchemy: the search for new superhard materials. MRS Bull. 1998;23:22–7.
39. Chen XQ, Niu H, Li D, Li Y. Modeling hardness of polycrystalline materials and bulk metallic glasses. Intermetallics. 2011;19:1275–81.
40. Tian Y, Xu B, Zhao Z. Microscopic theory of hardness and design of novel superhard crystals. Int J Refract Met Hard Mater. 2012;33:93–106.
41. Bello I, Chan CY, Zhang WJ, Chong YM, Leung KM, Lee ST, et al. Deposition of thick cubic boron nitride films: the route to practical applications. Diamond Relat Mater. 2005;143:1154–62.
42. Mirkarimi PB, McCarty KF, Medlin DL. Review of advances in cubic boron nitride film synthesis. Mater Sci Eng, R: Rep. 1997;21:47–100.

How to cite this article: Durandurdu M. Tetrahedral amorphous boron nitride: A hard material. *J Am Ceram Soc*. 2020;103:973–978. https://doi.org/10.1111/jace.16803